Mem. S.A.It. Vol. 74, 75

Memorie della

Investigating the Early Universe with the Cosmic Microwave Background Anisotropy

P. de Bernardis[1], P.A.R. Ade[2], J.J. Bock[3], J.R. Bond[4], J. Borrill[5], A. Boscaleri[6], K. Coble[7], C.R. Contaldi[4], B.P. Crill[8], G. De Troia[1], P. Ferreira[9], K. Ganga[10], M. Giacometti[1], E. Hivon[10], V.V. Hristov[8], A. Iacoangeli[1], A.H. Jaffe[11], W.C. Jones[8], A.E. Lange[8], L. Martinis[12], S. Masi[1], P. Mason[8], P.D. Mauskopf[2], A. Melchiorri[9], T. Montroy[7], F. Nati[1], C.B. Netterfield[13], E. Pascale[6], F. Piacentini[1], D. Pogosyan[4], G. Polenta[1], F. Pongetti[14], S. Prunet[4], G. Romeo[14], J.E. Ruhl[7], F. Scaramuzzi[12]

[1] Dipartimento di Fisica, Universita' La Sapienza, Roma, Italy
[2] Dept. of Physics and Astronomy, Cardiff University, Cardiff CF24 3YB, Wales, UK
[3] Jet Propulsion Laboratory, Pasadena, CA, USA
[4] Canadian Institute for Theoretical Astrophysics, University of Toronto, Canada
[5] National Energy Research Scientific Computing Center, LBNL, Berkeley, CA, USA
[6] IROE-CNR, Firenze, Italy
[7] Dept. of Physics, Univ. of California, Santa Barbara, CA, USA
[8] California Institute of Technology, Pasadena, CA, USA
[9] Nuclear and Astrophysics Laboratory, University of Oxford, Keble Road, Oxford, OX 3RH, UK
[10] IPAC, California Institute of Technology, Pasadena, CA, USA
[11] Astrophysics Group, Blackett Laboratory, Imperial College, London
[12] ENEA, Frascati, Italy
[13] Depts. of Physics and Astronomy, University of Toronto, Canada
[14] Istituto Nazionale di Geofisica, Roma, Italy

Abstract. Several experiments (including BOOMERanG, MAXIMA, DASI, VSA, CBI) have recently detected very low contrast structures in the Cosmic Microwave Background (CMB), the otherwise isotropic radiation coming from the early Universe. These structures have a contrast of the order of 25 ppm and a dominant angular size of one degree. In the current cosmological model, these structures result from acoustic oscillations of the primeval plasma within the horizon at recombination ($z \sim 1100$). In the framework of the Hot Big Bang theory with the inflationary hypothesis, the statistical properties of the image of the CMB allow us to measure most of the cosmological parameters.

Key words. Cosmology – Cosmic Microwave Background

1. CMB theory

In the framework of the Hot Big Bang model, when we look to the Cosmic Microwave Background we look back in time to the epoch when temperature decreased below 3000K for the first time: then hydrogen atoms formed from the primeval plasma and the universe became transparent (recombination). It is the end of the plasma era, at a redshift $\sim$ 1000, when the universe was $\sim$ 50000 times younger, $\sim$ 1000 times hotter and $\sim 10^9$ times denser than today (Gamow (1946), Weinberg (1977), Peebles (1994)). Photons generated in the early Universe are last scattered at recombination. Thereafter they travel free to our telescopes. Density perturbations $\Delta\rho/\rho$ were oscillating in the plasma era (as a result of the opposite effects of gravity and photon pressure). After recombination, density perturbations can grow and create the hierarchy of structures we see in the nearby Universe. CMB temperature fluctuations are closely linked to density fluctuations at recombination through three effects: the density fluctuation of the plasma of photons and matter in thermal equilibrium, the gravitational redshift of photon escaping from a density perturbation, and the Doppler effect of photons scattered by electrons with infall velocity v. In formulas $\Delta T/T = \Delta\rho/\rho/3 + \Delta\phi/c^2/3 - (v/c) \cdot n$. Mapping the CMB temperature we map the density and velocity fields in the Universe at recombination, and sample the direct result of early physical processes. In the primeval plasma, photons/baryons density perturbations start to oscillate only when the sound horizon becomes larger than their linear size. Small wavelength perturbations oscillate faster than large ones. The result is that perturbations with different linear size arrive at recombination with different phase. The largest ones have about the same size as the horizon at recombination: these have just enough time to arrive at recombination maximally compressed (or rarified). They produce a network of cold and hot spots in the image, with the dimensions of the acoustic horizon (similar to the causal one, since the sound speed is $\sim c/\sqrt{3}$). The presence of a characteristic dimension of the spots results in a peak in the angular power spectrum of the CMB image. The projected angular size of the horizon can be computed by means of the Friedmann equation as a function of the cosmological parameters. We expect a strong dependence of this observable from the density parameter, which controls the curvature of the Universe. In a super-critical density, positive curvature Universe, light rays from opposite sides of the perturbation converge towards the observer along curved geodesics: the same density perturbations will appear larger than in an Euclidean Universe. The reverse happens in a low density Universe with negative curvature. The computation shows that the result is mainly a function of two cosmological parameters, Ω_Λ and Ω_{Mo}, but the typical size of the horizon is always of the order 1^o. If $\Omega_\Lambda + \Omega_{Mo} = \Omega = 1$, then the dependence on the relative contributions of matter and vacuum is very weak, and the typical size of the horizon is $\theta_H \sim 0.85^o$. These spots produce a peak in the power spectrum at multipole $\ell_1 = \pi/\theta_H \sim 210$.

Smaller perturbations start to oscillate earlier and have more time to oscillate, so they can arrive at recombination with different phases. Also, they oscillate faster than large ones. Depending on the number of quarter periods they can undergo, they can arrive either with maximum compression (rarefaction) or with zero density contrast. We thus expect an approximately "harmonic" series of interleaved peaks and dips in the angular power spectrum of the CMB. In the adiabatic inflationary model, the relative amplitudes of the second to first peak is sensitive to the density of baryons Ω_{Bo} and to the spectral index n of the primordial density fluctuations spectrum, assumed of the form $P(k) \sim k^n$.

Send offprint requests to: P. de Bernardis
Correspondence to: Univ. La Sapienza, Dip. Fisica, P.le A. Moro 2, 00185 Roma, Italy

Detection of the third peak allows to remove the degeneracy between n and Ω_{Bo} and measure both (see Hu & Dodelson (2002) for a review of the theory of cosmological acoustic oscillations and Efstathiou & Bond (1999) for a discussion on the measurement of cosmological parameters from the angular power spectrum of CMB anisotropy).

The inflationary hypothesis (see e.g. Linde (2002), Kolb & Turner (1990)) is very appealing, because it explains the large-scale smoothness of the CMB by solving the paradox of horizons; it stretches the space to flat, so that $\Omega = 1$ naturally; it inflates quantum fluctuations from microscopic scales to cosmological scales, creating scalar and tensor fluctuations responsible for CMB anisotropies and for galaxy formation. Scalar (density) fluctuations are expected to be gaussian, adiabatic, and to have a Harrison-Zeldovich power spectrum $P(k) \sim k^n$ with $n \lesssim 1$. In this framework, the image of the CMB is an image of quantum fluctuations at energies of 10^{19} GeV, seen through the powerful microscope of the inflationary Universe. Measurements of the CMB can test the inflationary hypothesis in three ways: by measuring Ω, by measuring n, and by measuring the peculiar CMB polarization pattern due to tensor fluctuations (Kamionkowski & Kosowski 1998).

2. CMB experiments

Many experimental teams have actively worked on the measurement of the spectrum, of the anisotropy power spectrum and of the polarization of the CMB. The purely Planckian nature of the spectrum has been established by the FIRAS spectrometer on board of the COBE satellite (Mather et al. 1990) and by the rocket borne FTS (Gush et al. 1990). It is the proof of the cosmological nature of the CMB and of the Hot Big Bang theory proposed by Gamow in the 50s.

The intrinsic, faint, large scale anisotropy has been first detected by the DMR instrument on board of the COBE satellite (Smoot et al. 1992). Its low level and its power spectrum supported the inflationary hypothesis.

The detection of smaller (sub-horizon) structures in the CMB is a difficult experimental problem. The size of the observable temperature fluctuations is of the order of a few tens μK, while instrumental, local and astrophysical backgrounds can be as large as few K. The differences in spectral and angular distributions allow the experimentalists to separate the cosmological component from the contaminations, but elaborate modulation techniques are needed (Miller et al. (2001), Piacentini et al. (2002), Lee et al. (1999)). Interferometers directly sample the correlation function of the temperature fluctuations (White et al. 1999), while total power receivers sample the temperature map: the power spectrum is derived by first organizing the time-ordered observations in a map and then performing the harmonic analysis.

The degree and sub-degree-scale anisotropy has now been detected by several ground based and balloon-borne experiments. Only recently, however, it has been possible to first detect the presence of peaks in the power spectrum (Miller et al. (1999), Torbet et al. (1999), Mauskopf et al. (2000)), and to produce images where the sub-degree anisotropy is clearly visible (de Bernardis et al. (2000), Hanany et al. (2000), Netterfield et al. (2002), Leitch et al. (2001), Scott et al. (2002), Mason et al. (2002)). Further results are expected soon from ARCHEOPS (Benoit et al. 2001) and from the NASA satellite MAP (Page 2000).

3. BOOMERanG

The BOOMERanG experiment, a balloon-borne microwave telescope with cryogenic bolometric detectors, was flown on a long duration circum-Antarctic stratospheric balloon in 1998 (see fig. 1). Several aspects of the instrument have been described in Mauskopf et al. (1998), Masi et

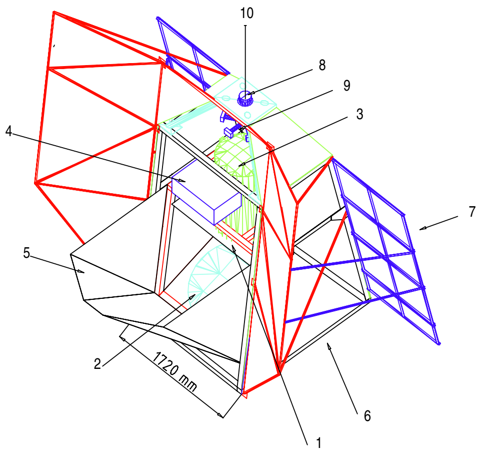

Fig. 1. The BOOMERanG payload. On the inner frame (1) are mounted the off axis primary mirror (2), the cryostat with the detection system (3), the analog electronics (4), the ground shield (5). On the outer frame (6) are mounted the sun shields, the solar panels (7), the azimuth pivot (8) with the flywheel (9). The pivot decouples the payload from the flight chain (10).

al. (1998), Masi et al. (1999), Piacentini et al. (2002), Pascale et al. (2002), Romeo et al. (2002), Crill et al. (2002). Modulation is achieved by scanning the sky at constant elevation and constant azimuth speed. The signal from the detector is AC coupled and high pass filtered. Since most of the contaminating signals are either constant or smooth in the sky, they are efficiently rejected by this modulation. The disadvantage of this technique is that it results in an anisotropic filtering of the sky maps, which has to be taken properly in account in the data analysis.

A further level of modulation comes from sky rotation. In fact, the central azimuth of the azimuth scans tracks the azimuth of the best sky region, a high latitude region about $30^o \times 40^o$ wide and free from cirrus dust, centered at coordinates $RA \sim 85^o$, $dec \sim -45^o$. Elevation is not changed during the scan, and is only changed in steps every several hours. The result of this strategy is that, due to sky rotation, the scans are gradually tilted in the sky, and the same pixel will be re-observed during the same day in differently tilted scans. This produces significant cross-linking in the sky coverage, which is important for the map-making algorithm used to create the image of the sky. The same process is repeated for several days. The comparison of maps obtained in different days, when the payload has drifted by thousands of km and the ground configuration is completely different, is a very effective tool to exclude contamination of the sky maps coming from signals in the telescope sidelobes.

The peak to peak length of our azimuth scans is $\Delta A \sim 60^o$, so that the scans in the sky have a length $\Delta\theta \sim \Delta A \cos e \sim 42^o$. This length has been selected as the best compromise between several factors: sky coverage, avoidance of the sun, repetition frequency of scans, detector's speed, 1/f knee in detectors noise, etc. As a result, our ℓ-space resolution is limited to $\Delta\ell \sim \pi/\Delta\theta \sim 4$. This is more than enough to resolve the acoustic peaks present in the power spectrum of the CMB anisotropy, which have a width $\Delta\ell_p \sim 100$ (Hu et al. 1997). In practice, we degrade the instrumental resolution to $\sim \Delta\ell_p/2$ by binning in ℓ, in order to improve the signal to noise ratio in each ℓ bin. The estimates of the power spectrum averaged over wide ℓ bins are called bandpowers. The finite length of the scans also limits the lowest multipole detectable $\ell_{min} \sim \Delta\ell$, but in practice a much higher $\ell_{min} \sim 25$ is set by the presence of drifts and $1/f$ noise. The maximum multipole observable in constant speed scans depends on the angular resolution of the telescope, on the time response of the detector (Hanany et al. 1998) and on its noise; in general the sensitivity of the instrument to different multipoles is described by a suitable window function taking into account these effects (see below). In the case of BOOMERanG $\ell_{max} \lesssim 1200$.

The BOOMERanG payload was flown by NASA-NSBF on Dec.29, 1998, from

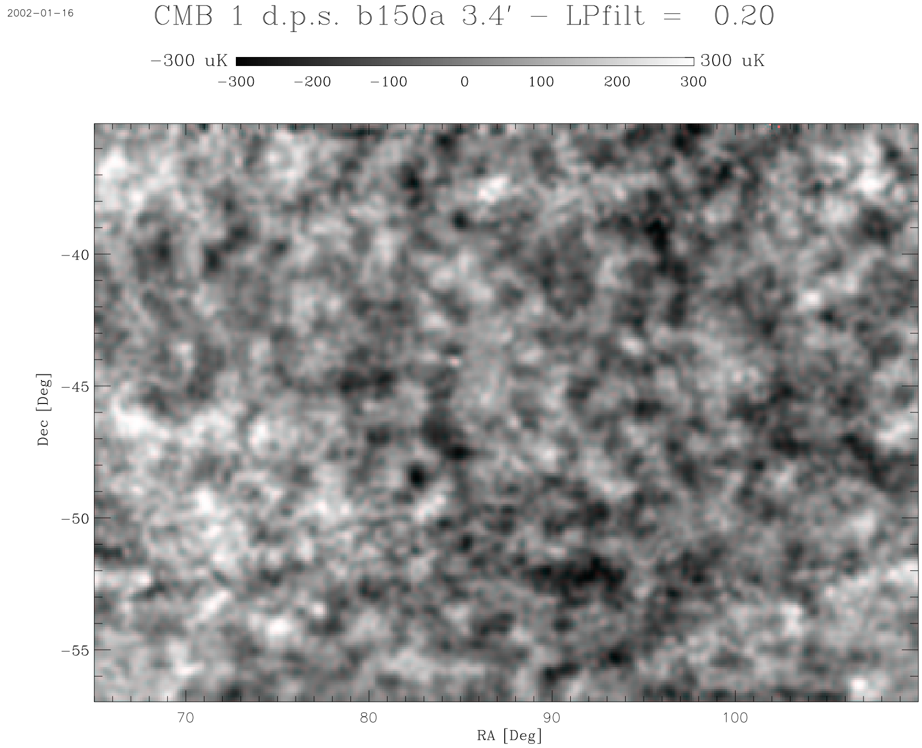

Fig. 2. Brightness fluctuations of the microwave sky at 150 GHz as measured by the BOOMERanG telescope. The brightness units are μK_{CMB}. The angular resolution of the telescope is 13' and the map has been smoothed with a 0.2^o FWHM gaussian kernel. Angular scales larger than $\sim 10^o$ have been removed from the image. In these units, the degree-scale fluctuations dominating the map have the same amplitude and shape as in the map at 90 GHz, proving that we are detecting anisotropies in the CMB, at scales similar to the causal horizon at recombination.

McMurdo (Antarctica). It remained at float for 10.6 days, circumnavigating Antarctica at an average altitude of 37 km. About 57 million 16-bit samples of the signal were collected for each of the 16 detectors. The data were edited for known instrument glitches, temperature fluctuations, and cosmic rays events. Less than 5% of the bolometer data has been found to be contaminated. Constrained realizations of noise were substituted to the contaminated signals.

The pointing has been reconstructed from the signals of the laser gyroscopes, of the differential GPS, and of the sun sensors. In the most recent pointing solution, repeated observations of compact sources show that the accuracy of the reconstruction is $\lesssim 2.5$ arcmin *rms*. Random errors in the pointing have the effect to smear-out the signals from small sources. This adds in quadrature to the intrinsic angular resolution of the telescope (9.5' FWHM at 150 GHz). The finite size of the pixelization has a similar effect. In ℓ space these three effects are modelled as a low pass filter, with a shallow cutting-off at about $\ell \sim 600$. The time-domain high pass filter mentioned above acts as a sharper high-pass at multipole $\sim$ 30. The result is a window function $W(\ell)$, which has to be taken into account in the reconstruction of the angular power spectrum of the sky. These effects limit the sensitivity of our observations at high multipoles. It can be shown that, for our particular scan strategy, the time-domain high pass filter acts as a high pass filter in the multipoles domain (Hivon et al. 2001). The result is that BOOMERanG is sensitive to a range of multipoles from $\ell = 50$ to $\ell = 1000$. Sky maps have been constructed from the time ordered data and pointing using four independent methods: naive maps (just coadding data on the same pixel); maximum likelihood maps obtained using the MADCAP package (Borrill 1999); maximum likelihood maps obtained using the iterative method of Natoli et al. (2001); suboptimal maps obtained using the fast map making method of Hivon et al. (2001). Degree-scale structures with amplitude of the order of $\sim 100\ \mu K$ are evident in the map at 150 GHz (see fig. 2). Consistent structure is also evident in the maps at 90 and 240 GHz. The similarity of the temperature maps obtained at different frequencies (de Bernardis et al. (2000)) is the best evidence for the CMB origin of the detected fluctuations. In fig. 3 we report a 3-D scatter plot of the 150 GHz channel vs the 90 GHz channel and the 240 GHz channel. The measured brightness fluctuations have been converted into temperature fluctuations of a 2.73K blackbody for all channels, and the slopes of the scatter plots are consistent with unity, thus confirming the origin of the signals.

Foregrounds contamination can be constrained significantly in the center of the observed sky region (de Bernardis et al. 2000), by comparison and correlation with dust templates (Masi et al. 2001). Moreover, at variance with Galactic maps, the fluctuations detected at 150 GHz pass several tests for gaussianity (Polenta et al. 2002). We can even set upper limits to non gaussian fluctuations mixed to the dominant gaussian ones: the rms amplitude of the non gaussian component should be less than a few % of the rms amplitude of the guassian one.

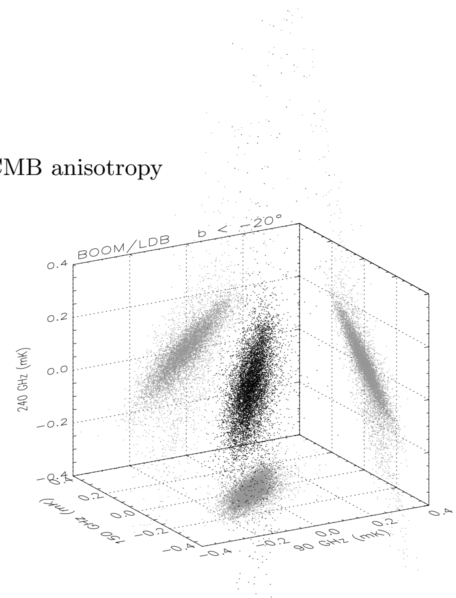

Fig. 3. 3D scatter plot of temperature fluctuations detected by BOOMERanG at 90, 150, 240 GHz. The measurements units are μK for thermodynamic temperature fluctuations of a 2.73K blackbody. The correlation shows that the bulk of the detected fluctuations has the spectrum of the CMB.

The gaussianity of the CMB temperature fluctuations is not trivial. As a matter of facts, if we do the gaussianity analysis on sky brightness data with the same angular resolution, but in different regions of the em spectrum, we do find important deviations from gaussianity. Our own 410 GHz channel is a good example of this behaviour (Polenta et al. 2002). The gaussian character of the fluctuations is telling us something important about the cosmological origin of the fluctuations, and is in good agreement with the predictions of the simplest inflationary models.

Gaussianity also insures us that all the information encoded in the map is provided by the angular power spectrum of the map. We have computed the power spectrum of the sky by means of independent methods (Borrill (1999), Hivon et al. (2001)), which rigorously take into account the effects of system noise, incomplete sky coverage, time-domain filtering of the data, beam shape etc. The current best spec-

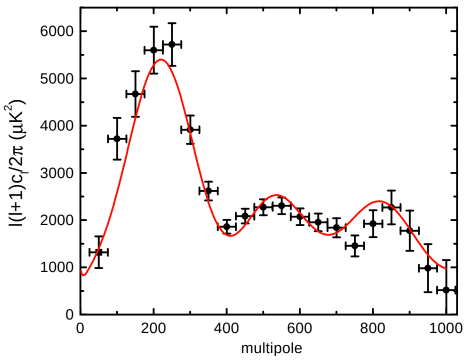

Fig. 4. Power spectrum of the CMB estimated from the combination of four independent 150 GHz maps of the sky measured by BOOMERanG

trum of the sky is obtained from a combination of four channels at 150 GHz, and is shown in fig. 4 (see Netterfield et al. (2002) for all the details of the analysis). In this spectrum, a peak at $\ell_{p1} \sim 213$ is evident at high statistical significance, and two further peaks at $\ell_{p2} \sim 541$, $\ell_{p3} \sim 845$ are also present at about 2σ significance (de Bernardis et al. 2002). They are interleaved with two dips at $\ell_{d1} \sim 416$ and $\ell_{d2} \sim 750$.

4. Impact of the BOOMERanG results on Cosmology

The simplest interpretation is that these features result from acoustic oscillations in the primeval plasma. The existence of these oscillations was predicted long time ago (Peebles et al. (1970),Sunyaev & Zeldovich (1970),Silk & Wilson (1980)), and is expected in the standard inflationary scenario (Bond & Efstathiou 1987). We derive the cosmological parameters within this theory framework, assuming adiabatic and gaussian initial density fluctuations. With this assumption a full database of power spectra can be built by allowing each of the cosmological parameters to cover a wide range of values. The spectra are computed using the programs CMBFAST and CAMB (Seljak and Zaldarriaga (1996), Lewis et al. (1999).

As explained in the introduction, the location of the first peak is directly related to the angular size of the acoustic horizon at recombination, and the comparison between linear and angular size of the horizon provides a clean way to measure Ω (Weinberg (2000) Melchiorri & Griffiths (2000)). In de Bernardis et al. (2000) we preliminarily derived Ω from the location of the first peak. We also derived a set of cosmological parameters by means of a bayesian analysis of the full power spectrum (for $\ell < 600$). While the results for Ω clearly indicated a flat geometry of the Universe, the results for other cosmological parameters (like $\Omega_b h^2$ and n_s were still affected by calibration errors and degeneracy of the spectra due to limited multipoles coverage. In subsequent papers we derived the cosmological parameters from the full power spectrum of BOOMERanG (up to $\ell \sim 1000$). This was derived from the final BOOMERanG maps, featuring improved beam and pointing reconstruction (Netterfield et al. (2002), de Bernardis et al. (2002)). The possibility to detect the third peak in the spectrum removed the degeneracy between $\Omega_b h^2$ and n_s. We find perfect consistency with a Euclidean Universe: $\Omega = 1.02^{+0.05}_{-0.06}$. This result is very important for cosmology, since pre-CMB estimates of Ω ranged from 0.3 to 1.2. If we trust General Relativity, the observation that $\Omega \sim 1$ today is very interesting. Our universe is following a very unstable solution of Einstein equations, and some mechanism (like inflation) has to be included in the standard Hot Big Bang scenario in order to explain this fact.

The second cosmological parameter well constrained by these data is the physical density of baryons: we find $\Omega_b h^2 = 0.022^{+0.004}_{-0.003}$. The density of baryons affects the symmetry of acoustic oscillations before recombination, thus controlling the ratio between even and odd order peaks in the power spectrum. The density of baryons also controls the nuclear reac-

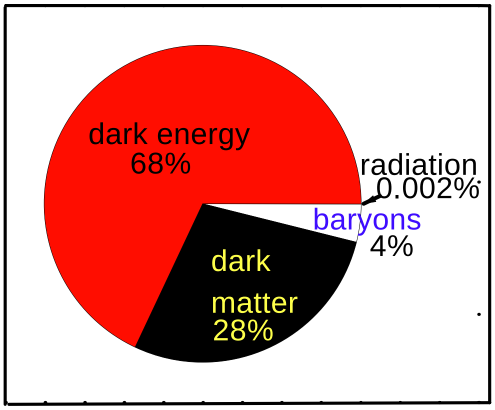

Fig. 5. Composition of the Universe from current CMB data and other cosmological evidence

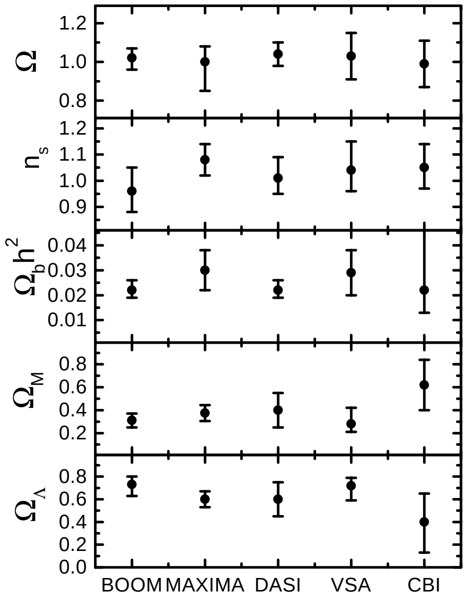

Fig. 6. Estimates of the main cosmological parameters from five independent CMB anisotropy experiments (plus COBE).

tions happening in the first minutes after the Big Bang and producing the light elements. Measurements of the primordial abundance of elements allow to estimate $\Omega_b h^2$ with still higher precision. Recent observations of primordial deuterium from quasar absorption line systems suggest a value $\Omega_b h^2 = 0.020 \pm 0.002$ at the 95 % C.L. (Burles et al. 2000). It is remarkable that such orthogonal techniques produce very consistent results: in our view it is a strong indication of the overall consistency of the hot big bang scenario.

The third parameter constrained is the spectral index of the power spectrum of primordial density perturbations. We find $n_s = 0.96 \pm 0.09$. In inflation models, the spectral index of the primordial fluctuations gives information about the shape of the primordial potential of the inflaton field which drove inflation. While there is no fundamental constraint on this parameter, the simplest models of inflation do give values that are just below unity.

Adding limited prior knowledge on the Hubble constant (i.e. $0.4 < h < 0.9$) and on the age of the Universe (i.e. $t > 10$ Gyrs) allows us to constrain significantly the density of dark matter (and of dark energy. The result is a universe where ordinary matter accounts for only 4% of the total mass-energy density, while about 25% of the Universe is in the form of still undetected dark matter. A mysterious form of dark energy (i.e. something with negative pressure in the stress-energy tensor) accounts for about 70% of the mass-energy density (see fig. 5).

5. Experimental and Cosmic Consistency

The power spectrum results from BOOMERanG have now been confirmed and extended by independent experiments. The measurements of MAXIMA, DASI, VSA, CBI (Leitch et al. (2001), Lee et al. (2002), Scott et al. (2002), Mason et al. (2002)) are all consistent with the power spectrum detected by BOOMERanG. Moreover, all these independent experiments find consistent estimates for the cosmological parameters (see fig. 6). The joint probability $P = \prod \mathcal{L}_i$ for these parameters are shown in fig. 7. The resulting estimates for the parameters are (at 95%

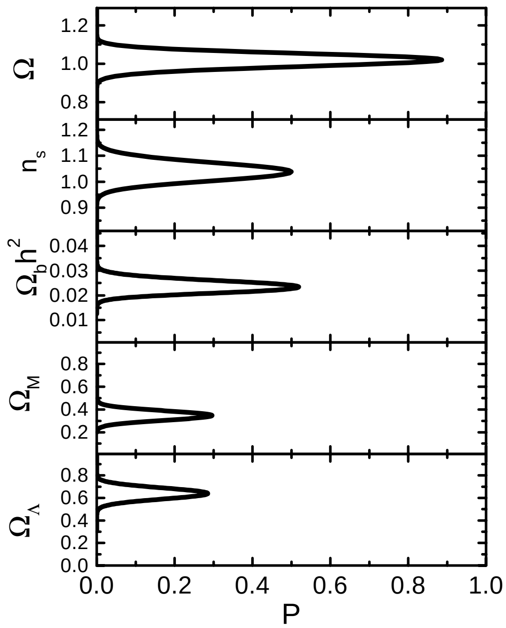

Fig. 7. Joint probability of each cosmological parameter given the estimates from COBE, BOOMERanG, MAXIMA, DASI, VSA, CBI.

confidence): $\Omega = 1.02^{+0.05}_{-0.06}$, $n_s = 1.04^{+0.04}_{-0.06}$, $\Omega_b h^2 = 0.023^{+0.005}_{-0.003}$, $\Omega_m = 0.35^{+0.07}_{-0.08}$, $\Omega_\Lambda = 0.64^{+0.08}_{-0.10}$.

We are neglecting here the fact that all these experiments are analyzed in combination with the same COBE data at low multipoles to estimate the cosmological parameters. The rigorous combined estimate of cosmological parameters from five of the six CMB experiments mentioned above is in Sievers et al. (2002), with results very similar to the ones reported here.

The apparently strange composition of the Universe is confirmed by independent cosmological observations (see e.g. Perlmutter et al. (1997, 1998); Garnavich et al. (1998); Riess et al. (1998)) and remains one of the most important open questions in cosmology and fundamental physics.

6. The Future

CMB experiments can improve our understanding of Nature in several ways. We will not even start to say how much the two CMB space mission (the ongoing MAP of NASA and the incoming Planck of ESA) will impact cosmology. They will provide full sky maps free of systematic effects, with high resolution, wide frequency coverage, and precise calibration, resulting in precision measurements of the CMB power spectrum and of the cosmological parameters. CMB Polarization measurements like the ones carried out by the new BOOMERanG payload (see e.g. Masi et al. (2001a), Masi et al. (2001b)) will confirm the origin of the anisotropy and provide evidence for the type of perturbations (adiabatic vs isocurvature, for example) responsible for the inital density fluctations. A subsequent generation of polarization experiments will provide deep insight on the physics of inflation (see e.g. Kamionkowski & Kosowski (1998)).

Acknowledgements. The BOOMERanG experiment is supported in Italy by Agenzia Spaziale Italiana, Programma Nazionale Ricerche in Antartide, Universita' di Roma La Sapienza; by PPARC in the UK, by NASA, NSF OPP and NERSC in the U.S., and by CIAR and NSERC in Canada.

References

Benoit A., et al., Astroparticle Phys., in press, 2001, astro-ph/0106152

Bond, J.R. & Efstathiou, G. 1987, Mon. Not. R. Astron. Soc. 226, 655

Borrill, J., in 3K Cosmology astro-ph/9911389

Burles, S., Nollett, K.M. & Turner, M.S. 2000, astro-ph/0010171

Crill B., et al., astro-ph/0206254

de Bernardis, P., et al. 2000, Nature, 404, 955-959

de Bernardis, P., et al. 2002, Ap.J. 564, 559-566, astro-ph/0105296

Efstathiou G., and Bond, J. R., 1999, MNRAS, 304, 75

P.M. Garnavich et al. 1998, Ap.J. Letters 493, L53;
Gamow G., 1946, Phys.Rev., 70, 572
Gush H.P. et al., 1990, Phys. Rev. Lett., 65, 537
Hanany S., Jaffe A., Scannapieco E., 1998, MNRAS 299, 653-660, astro-ph/9801291
Hanany, S. et al., 2000, Ap.J., 545, L5-L9
Hivon E. et al., 2001, astro-ph/0105302
Hu W., Sugiyama N. & Silk J., 1997, Nature, 386, 37
Hu, W., & Dodelson, S., ARAA, 2002 (astro-ph/0110414).
Kolb E.W. and Turner M.S, 1990, The Early Universe, Addison-Wesley
Kamionkowski M., Kosowski A., Phys.Rev.D., 67, 685, (1998)
Lee A., et al., 1999, in "3K cosmology", AIP Conf. Proc. 476; astro-ph/9903249
Lee A., et al., 2002, submitted to Ap.J., astro-ph/0104459
Leitch E.M., et al., 2001, astro-ph/0104488
Lewis A., Challinor A., Lasenby A., astro-ph/9911177 (1999)
Linde A., 2002, Stephen Hawking's 60th birthday conference, Cambridge University, Jan. 2002 hep-th/0205259
Masi S., et al., Cryogenics, 38, 319-324 (1998)
Masi S., et al., Cryogenics, 39, 217-224 (1999)
Masi S., et al., Ap.J, 553, L93-L96, 2001, astro-ph/0101539
Masi S., et al., in Astrophysical Polarized Backgrounds, AIP Conf. Ser. 609, pg. 122-127; Cecchini, Cortiglioni, Sault and Sbarra eds. (2001a)
Masi S., et al., in Experimental Cosmology at Millimetere Wavelengths, 2K1B2, AIP Conf. Ser. 616, 168-174, De Petris and Gervasi eds.(2001b)
Mason B., et al., 2002, submitted to Ap.J., astro-ph/0205384; Pearson T.J., et al., 2002, submitted to Ap.J., astro-ph/0205388.
Mather J., et al., 1990, Ap.J., 354, L37
Mauskopf P., et al., Applied Optics 36, 765-771, (1997)
Mauskopf P., et al., 2000, Ap.J., 536, L59-L62
Melchiorri A. and Griffiths L.M., astro-ph/0011147, (2000)
Miller, A. et al. 1999, Ap.J., 524, L1
Miller, A. et al. 2001, astro-ph/0108030
Natoli P., et al. 2001, submitted to Ap.J., astro-ph/0101252
Netterfield B., et al., 2002, Ap.J., in press, astro-ph/0104460
Page L., 2000, Proc IAU Symposium 201 Eds A. Lasenby & A. Wilkinson, astro-ph/0012214
Pascale E., and Boscaleri A., in BC2K1, AIP Conf. Ser. 616, De Petris and Gervasi eds.
Peebles P.J.E, 1994, Principles of Physical Cosmology, Princeton Series in Physics
Peebles, P.J.E, and Yu, J.T. 1970, Ap.J. 162, 815
Perlmutter, S. et al. 1997, Ap. J. 483, 565;
S. Perlmutter et al. 1998, Nature 391, 51;
Piacentini F., et al., Ap.J.Suppl. 138, 315-336, (2002) astro-ph/0105148
Polenta G., et al., Ap.J.Letters in press, astro-ph/0201133
Pryke C., et al., astro-ph/0104490
A.G. Riess et al. 1998, Ap. J. 116, 1009
Romeo G., et al., in BC2K1, AIP Conf. Ser. 616, De Petris and Gervasi eds.
Scott P.F., et al., 2002, MNRAS, submitted, astro-ph/0205380
Seljak U., Zaldarriaga M., Astrophys.J. , 469, 437, (1996)
Sievers J.L., et al., 2002, submitted to Ap.J., astro-ph/0205387
Silk J. & Wilson M. L. 1980, Physica Scripta, 21, 708
Smoot G., et al., 1992, Ap.J.,1992, 396, L1
Sunyaev, R.A. & Zeldovich, Ya.B., 1970, Astrophysics and Space Science 7, 3
Torbet E., et al., 1999, Ap.J., 521, L79-L82
Weinberg S., 1977, The first three minutes, Basic Books, ISBN-0465024378
White M., et al., astro-ph/9912422
Weinberg S., Phys.Rev. D62, 127302, (2000)